THE AMERICAN SOCIETY OF MECHANICAL ENGINEERS
345 E. 47 St., New York, N.Y. 10017

86-GT-137

Friction Damping in Compressor Blade Dovetail Attachments

J. M. ALLEN
Westinghouse Electric Corporation
Combustion Turbine Engineering Department
Concordville, Pennsylvania 19331

ABSTRACT

An empirical model is presented for predicting the fundamental mode resonant response of friction damped, free standing compressor blades from the cyclic slip that can occur in its dovetail attachment. The model is an extension of the conventional approach in that it includes the microslip regime of slip by assuming that the tangential force coefficient (tangential force to normal force ratio when slip occurs) depends on the magnitude of slip but, like friction coefficient, is independent of normal force. Experimental data obtained from bench damping tests are presented relating these quantities for plain and coated [copper-nickel indium (Cu-Ni-In) plus molydisulphide (MoS_2)] dovetail attachments. The results demonstrate that substantial friction damping can be obtained at low compressor speeds, where aerodynamic excitation is often most severe, and that such damping is dominated by the microslip properties of the dovetail interface. The dovetail coating significantly increased friction damping and proved to be durable in an endurance test, as it has in service.

NOMENCLATURE

(ASF) = hysteresis loop area shape function

E_f = energy dissipated per cycle of vibration by slip in the dovetail attachment

$\bar{F}$ = generalized exciting force amplitude

$\bar{m}$ = generalized mass

M_s = instantaneous vibratory bending moment about root axial centerline when slip occurs in the dovetail attachment

$\bar{M}$ = vibratory moment amplitude

$\bar{M}_s$ = vibratory moment amplitude when slip occurs

$\bar{M}_o$ = vibratory moment amplitude when no slip occurs

n = exponent in power function equation relating slip and tangential force coefficient

N_ℓ, N_r = normal reactions on left and right flanks of dovetail

P = clamping load

$\bar{q}$ = generalized displacement amplitude

$\bar{q}_s$ = generalized displacement amplitude when slip occurs

$\bar{q}_o$ = generalized displacement amplitude when no slip occurs

R = moment arm distance on dovetail root

RPM = turbine rotational speed, revolutions per minute

s = slip

α = dovetail flank angle

δ = damping logarithmic decrement

δ_s = damping logarithmic decrement due to slip in the dovetail attachment

δ_o = damping logarithmic decrement when no slip occurs

ΔS = double amplitude of slip in a cycle of vibration

π = 3.14159

μ = tangential force coefficient (ratio of tangential to normal force when slip occurs)

$\bar{\mu}$ = tangential force coefficient at the extremes of a vibration slip cycle

μ_f = dynamic coefficient of friction (tangential force coefficient when macroslip occurs)

ω = natural circular frequency

Presented at the International Gas Turbine Conference and Exhibit
Dusseldorf, West Germany—June 8-12, 1986

INTRODUCTION

Large, land based combustion turbines are principally used to generate electrical power and, consequently, run at constant speed. This makes it possible to tune resonant frequencies of the compressor blading away from engine order excitations that could stimulate resonant modes of vibration and cause fatigue failure. However, resonance due to engine order wake excitations, and to non-engine order excitations from flow instabilities at low speed, cannot be avoided during startup and shutdown. Therefore, units frequently started for peak load generation can accumulate millions of high vibratory stress cycles and fatigue failures may result after a large number of starts (several hundred to a few thousand).

In order to withstand these low speed resonances, compressor blading must be designed with sufficient stiffness and damping to keep stresses below the endurance limits of the blade and disc materials. One means of providing additional mechanical damping is through slip in the dovetail attachment. It has been demonstrated that considerable damping occurs by this mechanism at low rotating speeds (1, 2); however, at full speed, centrifugal forces are so high that the oscillatory bending moment required to initiate slip in the dovetail may be larger than that required to fatigue the airfoil, which will usually be the case for blading in the early stages of compressors.

In this paper, an empirical model is presented for predicting the fundamental mode resonant response of friction damped, free standing compressor blades from the cyclic slip that can occur in its dovetail attachment. The model is an extension of the conventional approach in that it empirically allows for a difference in behavior in the microslip and macroslip regimes of slip. This is accomplished by treating the tangential force coefficient (tangential force to normal force ratio when slip occurs) as a function of the magnitude of slip, but - like friction coefficient - it is assumed to be independent of the normal force. Hence, the model reduces to the classical approach to friction damping analysis when the tangential force coefficient is independent of slip.

Results from friction damping experiments on compressor blades are presented which indicate that the amplitudes of slip associated with relatively large values of dovetail friction damping (say 10% logarithmic decrement) are in the microslip regime or in the transition regime between microslip and macroslip. Hence, it is important to account for the interface behavior associated with micro amplitudes of slip in practical friction damped response calculations.

The test data were obtained from friction damping bench tests of actual blades and disc sectors in which clamping loads, cyclic slip, and resonant vibratory stresses representative of those that could occur in service were applied. Two interface surface conditions were evaluated: a plain 12 percent chrome blade dovetail against a plain low alloy steel disc groove and a copper-nickel indium (Cu-Ni-In) and molydisulphide (MoS_2) coated dovetail against a shot peened groove.

While friction damping is obviously beneficial from the point of view of limiting resonant vibration, Lazan (3) has pointed out that "a joint optimized for maximum dry-slip damping is generally subject to serious fretting and corrosion effects... and may also initiate fatigue cracks... the cure may, therefore lead to problems worse than the original problem." The fretting fatigue problem is not uncommon in the gas turbine industry. In compressors of units employed in electric power peaking service, fretting damage on the contact surfaces has at times resulted in fretting fatigue after many starts. Clearly then, the fretting fatigue problem must be given equal consideration if friction damping is to be successfully employed in preventing vibration failure. In this regard, limited durability testing of each surface condition was also conducted in the same blade vibration test apparatus, and these results are also presented, as well as a brief discussion of service experience with these interfaces.

DOVETAIL FRICTION DAMPING MODEL

Criterion for Slip

For friction damping to occur, there must be relative motion between mating surfaces. For the fundamental bending mode of vibration, the forces and reactions on the dovetail when slip occurs may be approximated by the two dimensional representation shown in Figure 1. The equations of equilibrium for the system of forces shown are

$$(\text{Sin}\alpha - \mu\text{Cos}\alpha)N_\ell - (\text{Sin}\alpha + \mu\text{Cos}\alpha)N_r = 0, \tag{1}$$

$$(\text{Cos}\alpha + \mu\text{Sin}\alpha)N_\ell + (\text{Cos}\alpha - \mu\text{Sin}\alpha)N_r = P, \tag{2}$$

$$\mu(N_\ell + N_r)R = M_s \,. \tag{3}$$

Equations (1) - (3) are subject to the limitation that

$$\text{Tan}\alpha > \mu, \tag{4}$$

because if the tangent of the flank angle is less than the tangential force coefficient the reaction N_r becomes negative, which is physically impossible.

Solving equations (1) and (2) simultaneously for N_l and N_r and substituting the results into equation (3) yields

$$M_s = \frac{\mu}{1 + \mu^2}\frac{PR}{\text{Cos}\alpha}\,. \tag{5}$$

Equation (5) defines the vibratory moment M_s to cause relative motion between the blade and disc groove dove-

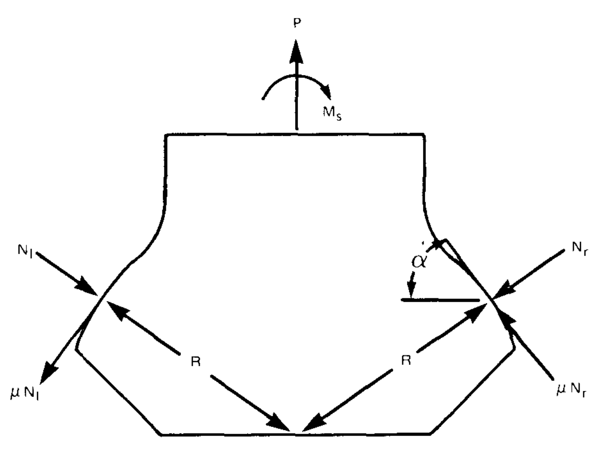

Fig. 1 - Applied and reaction forces on compressor blade dovetail during slip

tail contact surfaces for a given clamping load and tangential force coefficient. It also shows that the exciting force necessary to produce slip increases almost linearly with tangential force coefficient when its value is less than .5, whereas for values around 1.0 the effect of an incremental change is small. For example, increasing tangential force coefficient from .80 to 1.0 increases M_s by only 2.5 percent.

The tangential force coefficient, unlike friction coefficient, is a variable which depends on the elastic properties of the interface and the friction coefficient. For small amplitudes of slip (microslip), the tangential force coefficient will be less than the coefficient of friction, because the tangential force is partially resisted by elastic deformation of asperities in regions where slip has not yet occurred (4). When the amplitude of slip reaches a sufficiently large magnitude, gross slip (macroslip) occurs, and the tangential force coefficient becomes constant and equal to the friction coefficient (4).

An idealized mechanical model of interface elastic-plastic behavior is shown in Figure 2. In this model, macroslip occurs when the tangential force

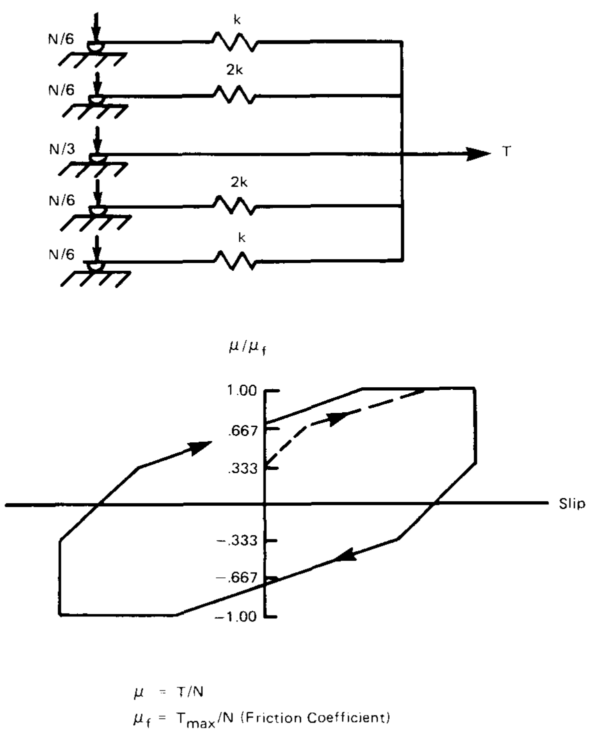

Fig. 2 - Spring-slider model illustrating dependence of tangential force coefficient (μ) on slip under monotonic and fully reversed loading conditions

equals the total normal force N times the friction coefficient. However, the rigid slider starts to slip, i.e., microslip initiates, when the tangential force coefficient is only one third of the friction coefficient. As the tangential force T increases further, tangential force coefficient continues to increase, and the two sliders next to the rigid one begin to slip when the tangential force coefficient is two thirds of the friction coefficient. All five sliders slip when the tangential force coefficient attains its maximum value, the value of the friction coefficient.

Relationship Between Tangential Force Coefficient and Slip

When the tangential force is cycled between fixed limits, equal in magnitude but opposite in sign, a hysteresis loop will develop as shown in Figure 2. The area of the hysteresis loop represents the energy loss due to friction. For the compressor blade dovetail, the vibrational energy dissipated by friction per cycle of vibration is

$$E_f = \frac{1}{R} \oint M_s ds$$
$$= \frac{2}{R} \int_0^{\Delta S} 2M_s ds - \frac{2\bar{M}_s}{R}(\Delta S), \tag{6}$$

where M_s is the instantaneous bending moment, ds is the incremental slip, and $2\bar{M}_s$ and ΔS are the maximum minus minimum values of bending moment and slip. Equation (6) can also be written in the form

$$E_f = \frac{2\bar{M}_s}{R}(\Delta S)\left[2\int_0^1 \frac{M_s}{\bar{M}_s}\, d\eta - 1\right], \tag{7}$$

where

$$d\eta = \frac{ds}{\Delta S}. \tag{8}$$

The integral on the right hand side of Equation (7) has values between .50 and 1.0. When it is .50, the sum inside the brackets containing the integral term is zero, which means that the area of the hysteresis loop is zero, and thus there is no friction damping. When the value of the integral is 1.0, the sum inside the brackets containing the integral term is 1.0, which means that the shape of the hysteresis loop is rectangular; this is the limiting or classical case where tangential force coefficient is constant and hence equal to the friction coefficient, regardless of slip amplitude. This sum then represents the shape function by which the area of a rectangle inscribing the hysteresis loop must be multiplied to obtain the energy dissipated by friction. It is, therefore, convenient to express Equation (7) in the form

$$E_f = \frac{2\bar{M}_s}{R}(\Delta S)(ASF), \tag{9}$$

where

$$(ASF) = \frac{2(1+\bar{\mu}^2)}{\bar{\mu}} \int_0^1 \frac{\mu}{1+\mu^2}\, d\eta - 1\,. \tag{10}$$

Equation (10) is equivalent to the sum inside the brackets in Equation (7), the difference being that Equation (5) has been substituted in order to express (ASF) in terms of tangential force coefficient. The variable μ represents the instantaneous tangential force coefficient in the slip cycle, while the variable $\bar{\mu}$ denotes its value at the extremes of the cycle.

In order to relate Equation (9) to friction damping, it is necessary to know the vibration energy input per cycle. Since free standing compressor blades are lightly damped, even when friction damping does occur in the dovetail attachment, the mode shape and natural frequency are essentially the same as in a free vibration calculation, and the energy supplied and dissipated per cycle of vibration can, therefore, be approximated (5) by the equation

$$\pi\bar{F}\bar{q} = \delta\bar{m}\omega^2\bar{q}^2, \tag{11}$$

where δ is the damping logarithmic decrement (which is dependent on amplitude of vibration when the damping is from friction), ω is the undamped natural circular frequency, $\bar{q}$ is the free vibration generalized displacement amplitude, $\bar{m}$ is the generalized mass, and $\bar{F}$ the generalized exciting force amplitude.

Slip damping can be measured in damping tests where the exciting forces are held constant and the clamping load varied until slip occurs. At sufficiently large clamping loads, slip is completely suppressed, and the damping will be entirely from sources other than friction. If the vibrating system is linear in the fully clamped condition, the generalized exciting force, from Equation (11), is

$$\bar{F} = \frac{\delta o\bar{m}\omega^2\bar{q}o}{\pi}. \tag{12}$$

When slipping occurs, the right hand side of (12) becomes

$$\bar{F} = \frac{(\delta o + \delta_S)\bar{m}\omega^2\bar{q}_S}{\pi}. \tag{13}$$

Equating (12) and (13) yields

$$\delta_s = \left[\frac{\bar{q}_o}{\bar{q}_s} - 1\right]\delta_o = \left[\frac{\bar{M}_o}{\bar{M}_s} - 1\right]\delta_o \,. \tag{14}$$

Substituting (14) into (11), with $\delta = \delta_s$, and equating the right hand sides of Equations (11) and (9) yields the desired relationship between cyclic slip and measured friction damping:

$$(ASF)(\Delta S) = \left[\frac{R}{2}\right]\left[\frac{\bar{m}\omega^2\bar{q}^2}{\bar{M}^2}\right]\left[1 - \frac{\bar{M}_s}{\bar{M}_o}\right](\delta_o M_o)\,. \tag{15}$$

In Equation (15), the first bracketed term on the right hand side is one half of the reaction moment arm on the dovetail (Figure 1), the second bracketed term is a constant for a given blade and mode of vibration and is determined by a free vibration modal analysis, the third bracketed term represents the reduction in vibration due to friction damping, and the fourth bracketed term is the product of logarithmic decrement and bending moment response when the dovetail is fully clamped. The friction damped stress ratio $\bar{M}_s/\bar{M}_o$ in Equation (15) is related to tangential force coefficient through Equation (5), hence, results from friction damping experiments can be plotted in terms of $(ASF)(\Delta S)$ versus $\bar{\mu}$ to obtain the desired correlation between tangential force coefficient and amplitude of slip.

MATERIALS AND EXPERIMENTAL PROCEDURE

Materials

The blade and disc materials evaluated and their room temperature tensile properties and fatigue endurance strengths are described in Table 1. The Cu-Ni-In and MoS_2 dry lubricant coating is described in Table 2.

Table 1
Blade/Disc Materials and Mechanical Properties

	Disc	Blade
Material	Low Alloy Steel	AISI 403 Steel
Composition (Wt. %)	3.5 Ni, 1.75 Cr, .5 Mo, .1 V, .4 C Max., .12 Si .3 Mn, Bal. Fe	12 Cr, .15 C, .60 Mn, .5 Si, .60 Mo, .6 Ni, .5 Cu, Bal. Fe
.2% Y.S.	140 - 155 ksi (965 - 1068 MPa)	80 ksi (551 MPa)
U.T.S.	150 ksi Min. (1034 MPa Min.)	100 ksi Min. (689 MPa Min.)
% R.A.	60 Nominal	60 Min.
10^8 ∿ Fatigue Strength	48 ksi (331 MPa)	60 ksi (413 MPa)

Table 2 - Interface Coating

Commerical Name	Composition (Wt. %)
Cu-Ni-Indium	58.5 Cu, 36.5 Ni, 5.0 In
Molydisulphide (Poxylube #750)	100% Epoxy Bonded MoS_2

The Cu-Ni-In coating was plasma sprayed onto a shot peened surface (.008-.010A, S170 steel shot). The molydisulphide was applied by spraying after which it was baked onto the surface for 30 minutes at approximately 400°F (204°C). Only the blade material was coated and dry film lubricated. Cu-Ni-In and MoS_2 thicknesses were nominally .003 inches (.0762 mm) and .0005 inches (.0127 mm), respectively.

Evaluation of the Cu-Ni-In plus MoS_2 coating was carried out on a single blade, the MoS_2 having been applied on top of the Cu-Ni-In. After the damping tests on the virgin coated blade were completed, the blade was resonated for six million vibration slip cycles, well beyond the point where mechanical behavior of the coated interface had stabilized. Damping and durability tests were then also conducted on the stabilized coated dovetail.

Experimental Apparatus

Friction damping was measured utilizing the blade-disc bench assembly shown in Figure 3. In this setup, the blade was driven by a Model A88 Calidyne, 100 lb. (445N) electromagnetic shaker. The shaker force was transmitted to the blade by a push rod, connected by studs to the shaker head and to a threaded boss brazed onto the blade near its tip. The blade was driven at the fundamental natural frequency of the blade-shaker vibratory system. This method of supplying excitation was chosen inasmuch as it was the only means available which was capable of providing a sufficiently large exciting force to obtain representative amplitudes of vibration in a blade of this size [11.8 inch (30 cm) height by 4.65 inch (11.8 cm) chord].

Blade response was measured with three strain gauges radially placed .5 inches (12.7 mm) above the

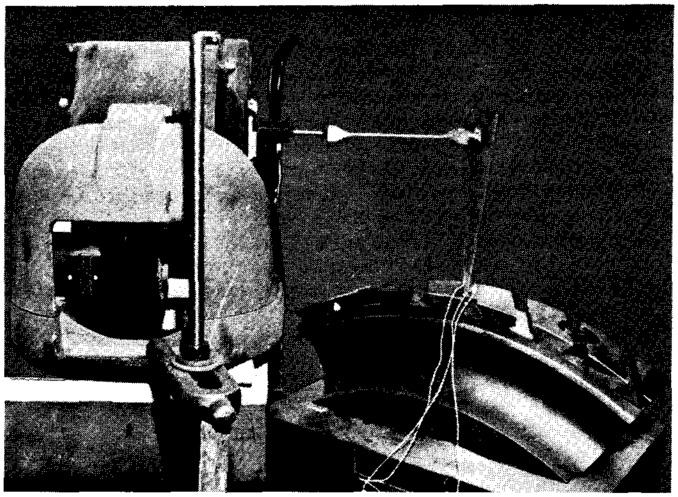

Fig. 3 - Friction damping and fatigue test apparatus

base of the airfoil. One gauge was located on the thickest part of the blade on its suction side (point of maximum stress when the blade vibrates in its fundamental mode), one was placed on the pressure side near the leading edge, and the third one on the trailing edge of the pressure side.

The blade was held in the middle groove of a 45 degree sector of compressor disc, which was fastened to a large block by two 8 inch (203 mm) long by 2 inch (50.8 mm) diameter socket head cap screws, as shown in Figure 4. The block was welded to a seismic table.

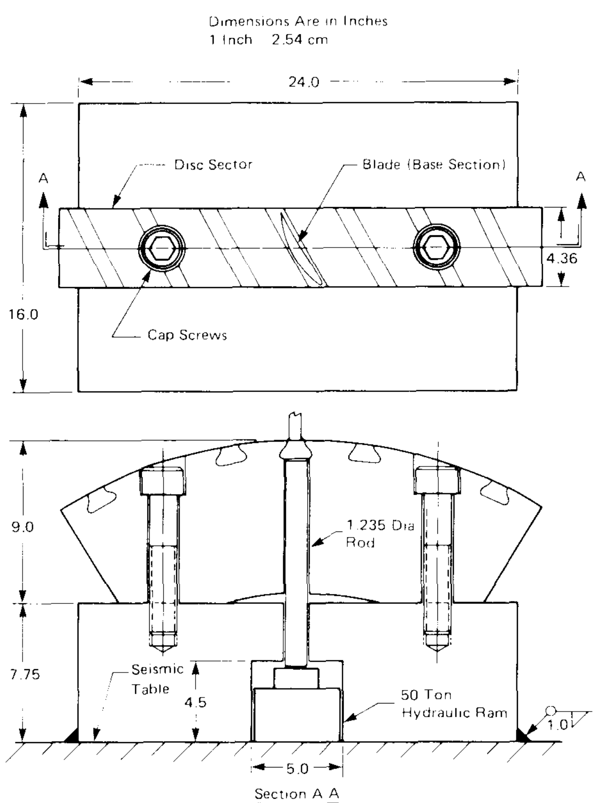

Fig. 4 - Friction damping and fatigue test fixture and static loading arrangement

Coaxial 1.25 inch (37.75 mm) diameter holes were drilled through the disc sector into the center of the middle groove bottom and through the block into a tunnel cutout on the underside of the block. A 11.6 inch (295 mm) long by 1.235 inch (31.37 mm) diameter rod was inserted at assembly for transmitting a clamping load P to the blade. The load P was supplied by a 100,000 lb. (.445 MN) capacity hydraulic ram located in the tunnel, Figure 4. The ram capacity well exceeded the maximum load that can be exerted by this blade in service, which is 71,200 lbs. (.317 MN) at an overspeed trip setting of 3960 RPM.

Although the clamping load P was applied to the root by the 1.235 inch (31.37 mm) diameter rod bearing against the bottom of the dovetail, it should be noted that no signs of slip, i.e., fretting, were observed in the contact region between the rod and dovetail when friction damping occurred. However, fretting was clearly evident on the flanks of the dovetail in these circumstances. Thus the test apparatus appears to have simulated actual dovetail joint slip behavior reasonably well.

Experimental Procedure

To measure friction damping, the system was tuned to resonate at a representative level of blade stress and the ram load varied to determine where slip occurs. When P was lowered enough for slip to commence, the blade stress diminished due to energy dissipation in the dovetail joint. The friction damped stress was recorded against clamping load P, from which the ratios $\bar{M}_s/\bar{M}_o$, $PR/\bar{M}_o \cos\alpha$, and $\bar{\mu}/(1+\bar{\mu}^2)$ were calculated. The corresponding values of (ASF) times cyclic slip were then calculated using Equation (15).

As stated earlier, Equation (15) requires that the damping logarithmic decrement under fully clamped conditions be independent of amplitude of vibration. In this case, the fully clamped damping was from two sources: the back electromotive force (back e.m.f.) in the shaker armature, which acts like viscous mechanical damping, and material damping which is dependent on stress level and distribution (6). However, in these experiments the magnitude of the back e.m.f. component of the damping logarithmic decrement (20 to 25 percent) was an order of magnitude larger than that from mechanical damping (on the order of two percent). Thus, the fully clamped logarithmic decrement, which was measured by the bandwidth method, was very nearly constant, as required by Equation (15).

Limited endurance testing of each surface condition was also conducted in the blade vibration test assembly.

RESULTS

Friction Coefficient

Data obtained following the procedures outlined above, for the three surface conditions, are plotted in Figure 5. In Figure 5, the friction damped stress ratio $\bar{M}_s/\bar{M}_o$ is plotted against dimensionless clamping load $PR/\bar{M}_o \cos\alpha$. Per Equation (5), the ratio of these two quantities is $\bar{\mu}/(1+\bar{\mu}^2)$ from which the tangential force coefficient can be calculated. For gross slip (macroslip) the ratio becomes $\mu_f/(1+\mu_f^2)$ and is the slope of the straight line between the origin and the onset of the knee (onset of microslip) in the curves in Figure 5. The coefficients of friction deduced by this means are approximately 1.0 for the plain dovetail, approximately .24 for the virgin coated dovetail, and nearly 1.0 for the stabilized coated dovetail.

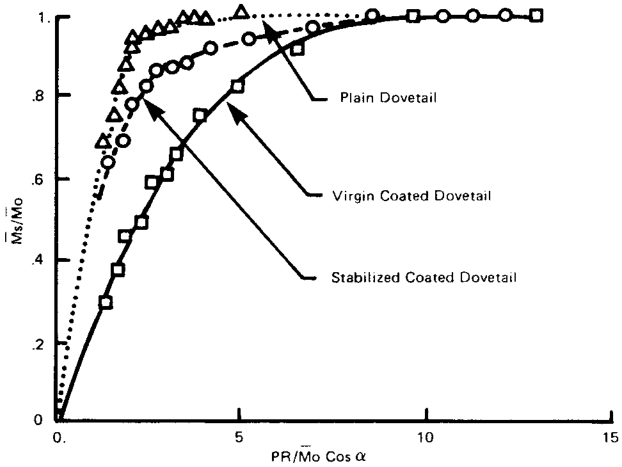

Fig. 5 - Friction damped stress ratio vs. dimensionless clamping load from bench tests of plain and coated dovetails

Tangential Force Coefficient vs. Amplitude of Slip

Values of (ASF)(ΔS) corresponding to the measured values of $\bar{M}_s/\bar{M}_o$ were calculated using Equation (15) and plotted against $\bar{\mu}/(1+\bar{\mu}^2)$ in Figure 6. Figure 6 shows that the relationship between $\bar{\mu}/(1+\bar{\mu}^2)$ and (ASF)(ΔS) is linear, on a log-log scale, in the microslip regime. Hence a power function fits the data satisfactorily in this domain. The evaluation of Equation (10) for a power function relationship between the variables yields the result

$$(ASF) = \frac{1 - n}{1 + n}, \tag{16}$$

where n is the exponent of the power law. From Figure 6, values of n are .273 for the plain interface, .318 for the virgin coated interface, and .500 for the stabilized coated dovetail. The corresponding area shape factors (ASF) are .571, .517, and .333. The relatively low value of (ASF) for the stabilized coated interface indicates that the corners of its hysteresis loop are significantly more rounded than for the plain and virgin coated interfaces. Because n is substantially higher (.500 vs. .273), tangential force coefficient for the stabilized coated dovetail is significantly less than for the plain dovetail in the microslip regime, Figure 6. The coefficient for the virgin coated dovetail is much less at all values of cyclic slip.

In the macroslip regime, the tangential force coefficient becomes constant and equal to the friction coefficient. For this case, Equation (10) can readily be evaluated utilizing bilinear log-log fits of the data, as shown in Figure 6. The result is

$$(ASF) = 1 - \frac{\Delta S_I}{\Delta S} \quad \frac{2n}{1 + n}, \tag{17}$$

where ΔS_I is the value of ΔS where the two lines intersect in Figure 6.

Using Equations (16) and (17), the area shape factors were computed for each data point, and in turn the value of cyclic slip for each data point was calculated. The results are plotted against tangential force coefficient in Figure 7. It can be seen that the tangential force coefficient becomes equal to the friction coefficient when cyclic slip exceeds 1.0 mils (25 μm) for the plain interface, 1.75 mils (45 μm) for the virgin coated interface, and about 3.0 mils (76 μm) for the stabilized coated dovetail.

Interface Durability

Plain Blade and Disc. After completion of the damping tests, an endurance test was run on the plain blade and disc. In these tests, no fretting or fatigue cracking was observed as long as PR/$\bar{M}_o$ Cosα was greater than 4.3 and the maximum airfoil stress/blade endurance strength ratio was less than .47; approximately 60 million cycles were accumulated under these conditions. However, as soon as the clamping was lowered to the point where friction damping was perceptible (PR/$\bar{M}_o$ Cosα = 2.1-2.7, maximum airfoil/endurance stress ratio = .44) fretting was observed as evidenced by a reddish brown debris (iron oxide) that continuously

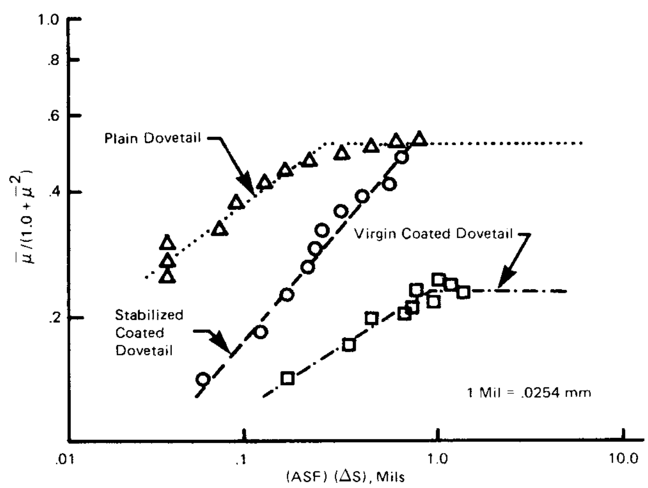

Fig. 6 - Relationship between tangential force coefficient ($\bar{\mu}$) and hysteresis area shape function times double amplitude of slip

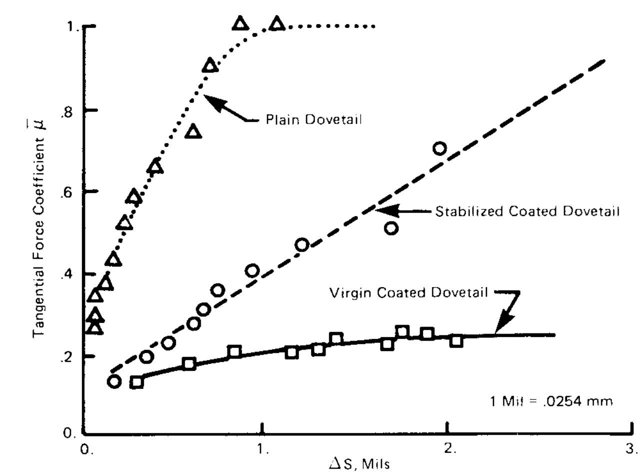

Fig. 7 - Tangential force coefficient ($\bar{\mu}$) as a function of double amplitude of slip

escaped from the ends of the dovetail and collected on the seal lands of the disc sector. (Subsequent examination of the dovetail surfaces revealed that the fretting occurred on the dovetail flanks; no evidence of fretting was observed on the bearing areas on the loading rod and bottom of the dovetail.)

A large disc fatigue crack was produced in less than 10 million fretting cycles under these conditions as shown in Figure 8. Close examination of the blade dovetail showed that it was also cracked. It is not known precisely when the cracks initiated, but none were noted in visual inspections after three and seven million cycles, however, these examinations were not sufficiently detailed to conclude that tight cracks were not present. The calculated cyclic slip associated with the failure ranges from .15 to .32 mils (3.8 to 8.1 μm). Such minute amounts of slip can cause large reductions in fatigue strength; Waterhouse (7) cites evidence that fretting fatigue damage may be maximum for double amplitudes of slip around .3 mils (7.5 μm) - very much in line with those associated with this failure.

Fig. 8 - Fretting fatigue crack in the disc after approximately 10 million cycles of the plain dovetail in the friction damping/fatigue test apparatus (Fig. 3)

Bending stress distributions at the base of the airfoil and root neck, from a finite element analysis, are shown in Figure 9. It can be seen that the maximum bending stress along the neck is 44 percent of the maximum airfoil stress. The peak root neck stress, which occurs at the uppermost point of contact between root and groove, was determined by a finite element contact analysis to be 2.6 times the nominal neck bending stress. Recalling that the airfoil/endurance stress ratio is .44, the peak stress as a fraction of endurance strength at the point of failure of the blade is estimated to be .44 x .44 x 2.6 = .50. The fretting fatigue strength reduction factor is, therefore, at least two for this combination of materials. It is likely that this factor is closer to three, in light of data reported by Fenner and Field (7), Jergeus and Johnson (8), and Hattori et. al (9). In any case, it is evident that while significant friction damping can occur at amplitudes of slip well below one mil (25.4 m), the benefits of the damping can be completely offset by large reductions in fatigue strength from fretting.

Dry Lubricant MoS_2. After slip data were obtained on the virgin Cu-Ni-In coated and MoS_2 lubricated blade, the dimensionless clamping load $PR/\bar{M}_o \cos\alpha$ was set at 2.27, which resulted in a resonant stress equal to one half the value that would have occurred had the root been rigidly clamped. The blade was then vibrated continuously for six million cycles (approximately 24 hours). After 100,000 cycles (24 minutes) the tangential force coefficient began to rise from an initial value of .24, and stabilized within one million cycles at a value of .430, Figure 10. This produced a decrease in damping, which resulted in a 60 percent increase in stress ($\bar{M}_s/\bar{M}_o$ increased from .51 to .82), while the double amplitude of slip decreased from 1.5 to 1.1 mils (38 to 28 μm). This change is attributed to cyclic expulsion of the dry lubricant MoS_2 from portions of the rubbing surfaces.

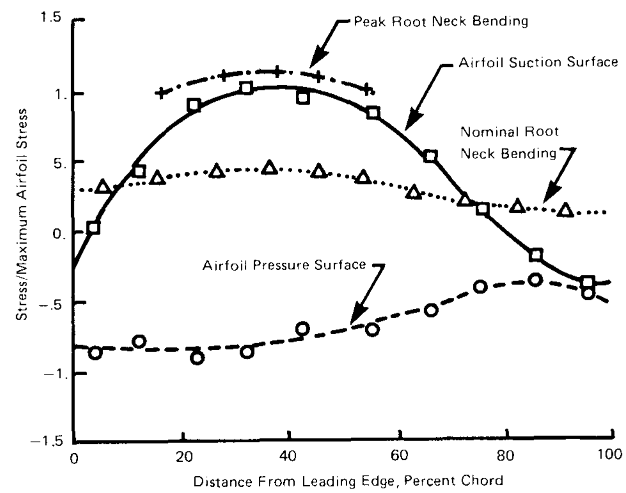

Fig. 9 - Fundamental mode vibratory stress distribution at base of airfoil and in the root neck from finite element analysis

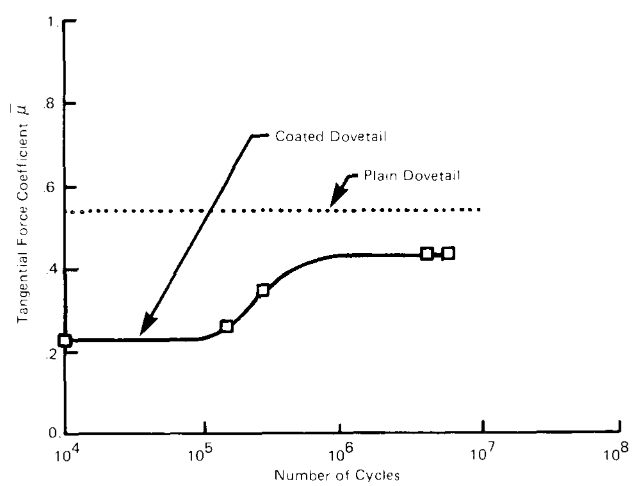

Fig. 10 - Effect of cycling on the tangential force coefficient for the Cu-Ni-In + MoS_2 coated dovetail

Cu-Ni-Indium Coated Dovetail. After the apparent removal of MoS_2 from portions of the rubbing surfaces during the aforementioned durability test, the stabilized coating was evaluated for its slip characteristics, as described earlier, and then durability tested at two stress levels. In both cases, clamping load was such that substantial slip occurred: .71 mils (18 μm) at the lower stress and .82 mils (21 μm) at the higher stress. The blade was initially vibrated at a maximum airfoil stress equal to 32 percent of the endurance strength, with $PR/\bar{M}_o \cos\alpha = 2.9$, for 77 million cycles and subsequently for 52 million more cycles at a maximum airfoil stress equal to 46 percent of the endurance strength - approximately the same as the failure stress for the uncoated blade - with $PR/\bar{M}_o \cos\alpha = 2.5$. No fretting fatigue cracking could be found, even though substantial fretting did occur on the uncoated disc. The Cu-Ni-In coating on the blade dovetail remained intact and showed minimal signs of wear.

Field Experience. The test blade and disc are from the third stage of the Westinghouse W501AA compressor that entered service around 1970. At that time, no surface treatment was given to blade dovetail or disc groove. About half of the 63 model W501AA compressor rotors in service developed high cycle fatigue cracks in the third stage. Most of the cracks occurred in the disc grooves with a few isolated instances of blade airfoil and dovetail cracking. Usually, less than 10% of the grooves were cracked, and the cracking was generally discovered after more than 500 starts were accumulated. No correlation with operating time at design speed could be found. Clearly, this was a problem of cumulative exposure to transitory excitation at low speeds and, hence, low clamping loads.

To solve the problem, the Cu-Ni-In coating and MoS_2 lubricant was introduced along with shot peening of the discs. In addition, the variable inlet guide vanes and increased interstage bleeding were employed to reduce rotating stall excitation. No fretting fatigue cracking has been observed since these modifications were introduced in the W501AA compressor in the mid to late 1970's, nor has it been observed in subsequent W501 models - comprising over 100 units - which use the same third stage blade. Thus, while the solution of the problem cannot be attributed entirely to the introduction of these surface treatments, it is reasonably certain that the coating significantly decreased the vibratory stress, due to increased friction damping, and that the fretting fatigue strength of the interface was improved. In any case, the field experience is consistent with the laboratory results.

DISCUSSION

The practical implications of the results from this study can best be demonstrated by an analysis that predicts dovetail damping behavior under turbine operating conditions for the surface conditions evaluated. The methodology is as follows:

1. Perform a free vibration analysis of the blade and calculate

$$\left[\frac{R}{2}\right]\left[\frac{\bar{m}\omega^2\bar{q}_o^2}{\bar{M}_o^2}\right](M_o\delta_o).$$

2. Assume several values of $\bar{\mu}/(1+\bar{\mu}^2)$ and pick off corresponding values of (ASF)(ΔS) from Figure 6.
3. Calculate the corresponding values of $\bar{M}_s$ using Equation (15).
4. Solve for corresponding clamping loads in terms of RPM, using Equation (5), and plot against $\bar{M}_s/\bar{M}_o$.
5. Repeat the process for as many exciting loads $\bar{M}_o$ and values of δ_o as desired.

Results obtained from following this procedure for an excitation that produces a bending moment response $\bar{M}_o$ equal to that required to fatigue the airfoil under fully clamped conditions are shown in Figure 11. The fully clamped logarithmic decrement assumed was .02. Figure 11 shows how the stress ratio $\bar{M}_s/\bar{M}_o$ increases as friction damping decreases with turbine speed. The

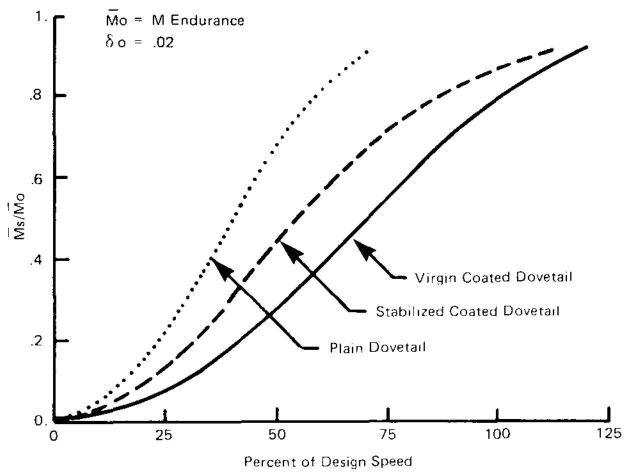

Fig. 11 - Calculated friction damped stress ratio as a function of design speed for the 3rd stage compressor blade in a 100 MW class combustion turbine

speed zone of greatest concern, with regard to stall excitation, usually falls in a range between one third and two thirds of design speed. The predicted reductions in stress at 50 percent of operating speed are 35% for the plain blade and groove, 58% for the stabilized coated dovetail and shot peened disc, and 74% for the virgin coated dovetail; in terms of logarithmic decrement, corresponding friction damping values are approximately 1%, 3% and 6%. These results demonstrate that significant friction damping is possible at low speeds, even in the early stages of compressors - the blade analyzed in this example is from the third stage of the 19 stage compressor in a 100MW class combustion turbine.

It is important to note that the amplitude of slip associated with relatively large amounts of friction damping (say 10%) is typically less than one mil (.0254 mm) - well within the microslip regime. This is demonstrated in Figure 12, where the friction damped stress ratios shown in Figure 11 are plotted in terms of amplitude of slip versus friction damping logarithmic decrement.

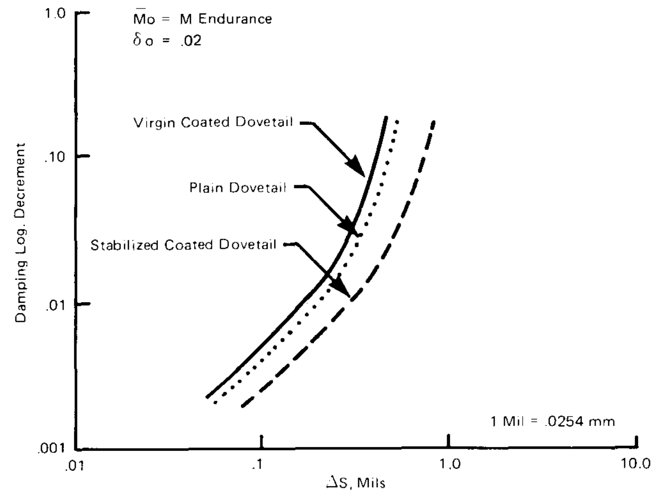

Fig. 12 - Calculated relationship between friction damping and double amplitude of slip for the 3rd stage compressor blade in a 100 MW class combustion turbine

SUMMARY AND CONCLUSIONS

An empirical model has been presented for predicting fundamental mode resonant response of friction damped, free standing compressor blades in which the microslip regime of slip is included and which reduces to the classical approach when tangential force coefficient is independent of the magnitude of slip. A dynamic bench test apparatus and procedure for generating the basic data required by the model has been described.

Significant reductions in vibratory stress can be obtained from friction damping in the microslip regime at low speed operation, where additional mechanical damping is most needed in combustion turbines subject to frequent starting and stopping. The Cu-Ni-In plus MoS_2 coating substantially increases friction damping compared to that obtainable in the plain dovetail attachment.

For conventional uncoated dovetails and grooves, the benefits of friction damping are apt to be offset by large reductions in fatigue strength from fretting associated with cyclic slip in the dovetail attachment. However, the coating has proven to be durable in endurance testing, as well as in service, and helpful in preventing fatigue failures.

ACKNOWLEDGEMENT

The author is indebted to his colleague Albert J. Marcellino for reviewing the manuscript and for numerous helpful suggestions and comments.

REFERENCES

1. Hanson, M. P., Meyer, A. J., and Manson, S. S., "A Method of Evaluating Loose-Blade Mounting as a Means of Suppressing Turbine and Compressor Blade Vibrations," Proceedings of S.E.S.A., Vol. 10, No. 2, pp. 103-116, 1953.

2. Hattori, T., Sakata, S., and Ohnishi, H., "Slipping Behavior and Fretting Fatigue in the Disk/Blade Dovetail Region," Paper No. 83 - Tokyo - IGTC-122, Tokyo International Gas Turbine Congress, October, 1983.

3. Lazan, B.J., "Damping of Materials and Members in Structural Mechanics," Pergamon Press, Oxford, 1968, pp. 23.

4. Bowden, F.P., and Tabor, D., "The Friction and Lubrication of Solids, Part I," Oxford University Press, 1953.

5. Den Hartog, J. P., "Mechanical Vibrations," McGraw Hill Book Co., 1956, pp. 133-134.

6. Lazan, B. J. and Goodman, L. E., "Material and Interface Damping," Shock and Vibration Handbook, Harris, C.M. and Crede, C.E. (eds.), McGraw-Hill, New York, 1961, Vol. 2, Chapter 36, 46 pp.

7. Waterhouse, R. B., "Fretting Corrosion," Pergamon Press, 1972, Chapter 8, pp. 130-144.

8. Jergeus H., and Johnson, A., "Fatigue Strength in Compressor Blade Attachments," Proceedings of the 14th International Congress on Combustion Engines (CIMAC), Helsinki, 1981, pp. GT29-1 to GT29-12.

9. Hattori, T., Nakamura, M., and Watanabe, T., "Fretting Fatigue Analysis by Using Fracture Mechanics," ASME Paper 84-WA/DE-10.